



Probabilistic Tsunami Hazard Analysis For Tuzla Test Site Using Monte Carlo Simulations

H. Basak Bayraktar^{1,2,3}, Ceren Ozer Sozdinler⁴

¹Department of Geophysics, Kandilli Observatory and Earthquake Research Institute, Bogazici University, Istanbul, 34684, Turkey

²Department of Physics “Ettore Pancini”, University of Naples Federico II, Naples, 80126, Italy

³Istituto Nazionale di Geofisica e Vulcanologia, Rome, Italy

⁴Institute of Education, Research and Regional Cooperation for Crisis Management Shikoku, Kagawa University, Takamatsu, 760-8521, Japan

10 *Correspondence to:* Hafize Başak Bayraktar (hafizebasak.bayraktar@unina.it)

Abstract. In this study, time-dependent probabilistic tsunami hazard analysis (PTHA) is performed for Tuzla, Istanbul in the Sea of Marmara, Turkey, using various earthquake scenarios of Prince Island Fault within next 50 and 100 years. Monte Carlo (MC) simulation technique is used to generate a synthetic earthquake catalogue which includes earthquakes having magnitudes between Mw 6.5 and 7.1. This interval defines the minimum and maximum magnitudes for the fault in the case of entire fault rupture which depends on the characteristic fault model. Based on this catalogue, probability of occurrence and associated tsunami wave heights are calculated for each event. The study associates the probabilistic approach with tsunami numerical modelling. Tsunami numerical code NAMI DANCE was used for tsunami simulations. According to the results of the analysis, distribution of probability of occurrence corresponding to tsunami hydrodynamic parameters are represented. Maximum positive and negative wave amplitudes show that tsunami wave heights up to 1 m have 65% probability of exceedance for next 50 years and this value increases by 85% in Tuzla region for next 100 years. Inundation depth also exceeds 1m in the region with probabilities of occurrence of 60% and 80% for next 50 and 100 years, respectively. Moreover, Probabilistic inundations maps are generated to investigate inundated zones and the amount of water penetrated inland. Probability of exceedance of 0.3 m wave height, ranges between 10% and 75% according to these probabilistic inundation maps and the maximum inundation distance calculated among entire earthquake catalogue is 60 m in this test site. Furthermore, at synthetic gauge points which are selected along the western coast of the Istanbul by including Tuzla coasts. Tuzla is one of the area that shows high probability exceedance of 0.3 m wave height, which is around 90%, for the next 50 years while this probability reaches up to more than 95% for the next 100 years.

1 Introduction

Marmara Region, especially highly populated cities along the coasts of the Marmara Sea, is the heart of Turkish economy in terms of having great number of industrial facilities in largest capacity and potential, refineries, ports and harbors. The Marmara Sea and the area is one of the most seismically active areas in Turkey and due to these circumstances, coastal cities in Marmara



region, especially Istanbul which has significant importance in terms of economy, and historical and sociocultural heritage with a population of more than 15 million, is under the threat of high damage due to possible big earthquake and also triggered tsunamis. Recent studies and evaluation of earthquake recurrence periods revealed that there is a high possibility of having an earthquake with magnitude larger than M_w 7.0 in Prince Islands fault. According to Ambraseys (2002), the latest earthquake on this fault system occurred in 1766 and since that time, this fault has been accumulating huge amount of energy. According to Parsons (2004), the probability of occurrence of $M > 7$ earthquake beneath the Marmara Sea was estimated to be 35-70% in the following 30 years in 2004. There has been a wide range of studies in Marmara Sea region regarding the fault mechanisms, seismic activities, earthquakes and triggered tsunamis. The region is attractive because of its complex structure and high possibility of an earthquake occurrence with the magnitude of larger than 7.0 offshore Istanbul mega-city.

The North Anatolian Fault Zone (NAFZ) controls the great part of the seismic activity in the Marmara Sea region. The fault zone sets apart Anatolia (Asian part of Turkey) and Eurasia due to the northward migration of Arabian Plate in the east and southward rollback of the Hellenic subduction zone in the west as seen in Fig. 1 (Armijo et al., 1999; Flerit et al., 2004; Le Pichon et al., 2015).

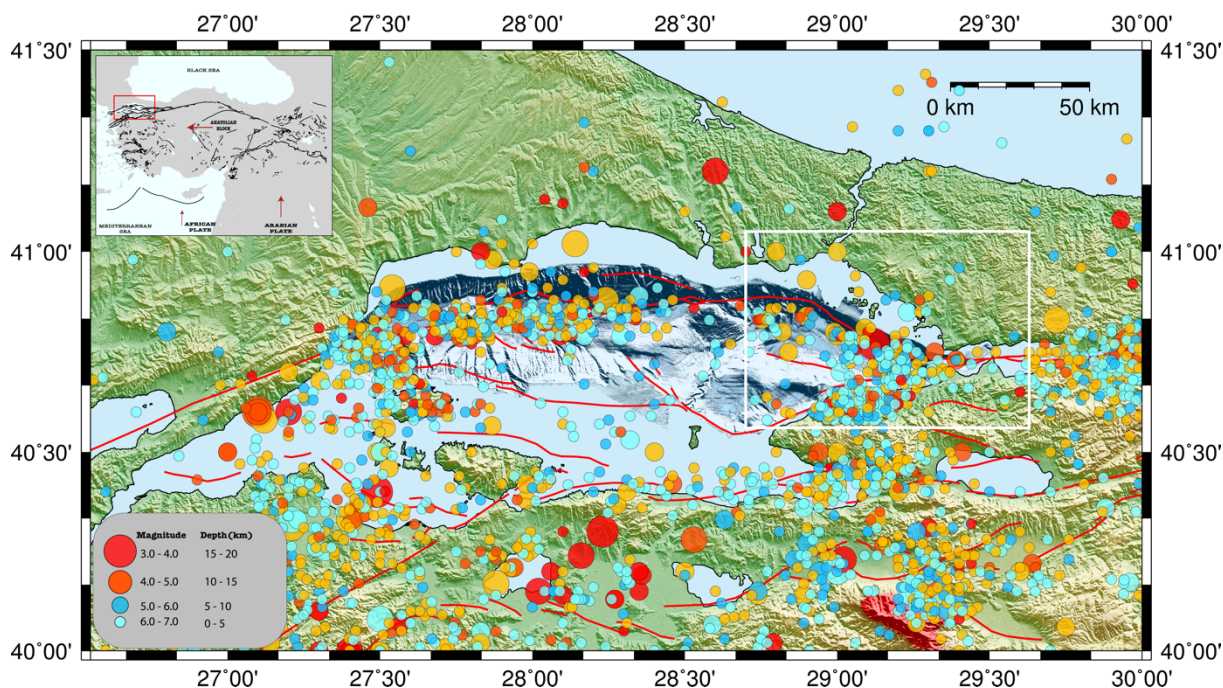


Figure 1: Seismicity map of the Marmara region and general tectonic map of the Turkey on the top – left. In the seismicity map, the size of the circles changes with magnitude of the earthquakes and the color of the circles defines the depth change of the earthquakes. Red lines show the known active faults (Modified from Emre et al., 2013) in the region and white square is the area with the PIF. In the general tectonic map of Turkey, red arrows show the direction of the plate motion, black lines show the active faults in the region (Modified from Emre et al., 2013) and red rectangular shows the Marmara region (created using The Generic Mapping Tools, Version 5.4.1).



The Marmara Sea region is a transition zone between the strike-slip regime of the NAFZ and the extension regime of the Aegean Sea area (on the top – left of Fig 1). The northern branch of the NAFZ forms a major transtensional NW- SE right bend under the Sea of Marmara at Çınarcık trough (Murru et al., 2016). The fault trace is attached to the complex Central Marmara and Tekirdağ pull-apart basins, before joining the NE-SW striking Ganos fault on land by following the northern margin of the Marmara Sea. Finally, the fault exits into the Aegean Sea by way of Saros Gulf (Wong et al., 1995; Armijo et al., 1999; Armijo et al., 2002; Okay et al., 1999; Le Pichon et al., 2001; Yaltirak 2002; McNeill et al., 2004). The fault trace beneath the Marmara Sea is not directly observable. Therefore, making a segmentation model for the offshore parts of the NAFZ is quite difficult (Aksu et al., 2000; Imren et al., 2001; Le Pichon et al., 2001; Armijo et al., 2002; Armijo et al., 2005; Pondard et al., 2007).

The current right-lateral slip rate along the NAFZ is about 25 mm/yr (Meade et al., 2002; Reilinger et al., 2006). In the western side, the motion between the Anatolia and Eurasia plates is accommodated across the Marmara region by ~ 19 mm/yr of right-lateral slip and 8 mm/yr of extension (Flerit et al., 2003; Flerit et al., 2004). Slip rates of the main Marmara fault ranging between 17-28 mm/yr (Le Pichon et al., 2003; Reilinger et al., 2006). On the other hand, Hergert and Heidbach (2010) suggests that the right-lateral slip rate on the main Marmara fault is between 12.8-17.8 mm/yr due to slip partitioning and internal deformation. The right-lateral slip rate for the PIF and Çınarcık basin is 15 ± 2 mm/yr and in addition to this, the fault has 6 ± 2 mm/yr of extension (Ergintav et al., 2014).

The main characteristic of the NAFZ is having earthquakes systematically propagated westward and historical records show that, northern strand of the NAFZ generates an earthquake with the recurrence interval of about 250 years beneath the Marmara Sea and the latest event occurred in 1766 (Ambraseys, 2002, Bohnhoff et al., 2013). This event caused the rupture of the 58 km long northern part of NAFZ from Izmit to Tekirdağ (Ambraseys and Finkel, 1995; Ambraseys and Jackson, 2000). However, the earthquake that happened on 2 September 1754 can be considered as the latest characteristic event for the Prince Islands segment and it caused the rupture of a 36 km long fault segment (Ambraseys and Jackson, 2000). The NAFZ has experienced two $M > 7$ earthquakes in August 1912 Ganos and August 1999 Izmit earthquakes recently. After the 1999 Izmit event seismic energy along the 150 km long northern part of the NAFZ, which extend right next to south of Istanbul beneath the Marmara Sea, has been accumulated continuously since 22 May 1766 earthquake and this situation increases the rupture possibility of the PIF and the risk for megacity Istanbul (Stein et al., 1997; Barka 1999; Bohnhoff et al., 2013). Ergintav et al., (2014) also indicated that the PIF segment is most likely to generate the next $M > 7$ earthquake along the Sea of Marmara segment of the NAF.

Beside these seismic activities in the region, studies on the historical tsunami records shows that 35 tsunami events happened between BC 330 and 1999 in the Marmara Sea region and the majority of them are earthquake-related tsunami events. 1509 earthquake, with an estimated magnitude around 8.0, is one of the examples for these events. This earthquake triggered a tsunami and the tsunami waves inundated along Istanbul coasts reaching the city walls and around 4000–5000 people died in the city (Ambraseys and Finkel, 1995). 1894 earthquake is also one of the important events that happened in Marmara Sea.



The earthquake triggered a tsunami and the sea inundated 200 m in Istanbul (Altinok et al., 2011). The recent one happened after the 17 August 1999 Izmit earthquake and after the earthquake, several small faults and submarine failures generated a tsunami. The International Tsunami Survey Team (Yalçiner et al., 1999; Yalçiner et al., 2000) investigated the region and they observed 2.66 m run-up along the coast from Tütüncüflük and Hereke and 2.9 m run-up at Değirmendere (Yalçiner et al., 90 2002).

Several tsunami hazard estimation studies were also conducted in the region. These tsunami analyses were mostly performed in deterministic manner using various earthquake scenarios depending on the combinations of different fault parameters without considering probability of occurrences. When focused on the 40 m long fault in Eastern Basin of Marmara Sea, maximum tsunami heights can reach 2 m along the Istanbul coast with locally considerable inundation, if this considered fault 95 has a significant normal component (Hebert et al., 2005). The rupture of Yalova Fault, Prince Island Fault or Central Marmara Fault can also cause a serious damage along the coast of Istanbul. Tsunami wave heights can reach 4.8m and can penetrate 340m from coast to inside in Haydarpaşa Port (Aytore et al., 2016).

A few number of probabilistic seismic and tsunami hazard analyses were also done in this region. Seismic hazard maps are prepared in the Marmara Sea region by describing fault segments and peak ground accelerations with the periods 100 corresponding to 10% and 2% probabilities of exceedance in 50 years (Erdik et al., 2004). Besides that, tsunami inundation maps are prepared based on probabilistic and deterministic analyses by depending on these segmentations (Hancilar, 2012). Time-dependent and time-independent earthquake ruptures are also estimated in the Marmara Sea region for next 30 years (Murru et al., 2016). These previous studies have been conducted for entire Marmara Sea region and therefore they give general and rough information about probability of occurrence in the region without focusing on any specific region 105 in high resolution. However, probabilistic tsunami hazard assessment is important, because it considers all possible earthquakes in a fault even they occur with very low probability and when decision makers design coastal zones and structures, especially critical ones, they would consider the results of probabilistic studies. Different from previous probabilistic approaches in Marmara Sea, in this study tsunami hazard assessment is done in the light of high possibility of occurrence of a big earthquake in Marmara Sea in the case of PIF rupture. The probability of earthquake occurrences in Prince Islands fault are taken into 110 account for the preparation of high-resolution tsunami inundation maps and distribution of hydrodynamic parameters due to the probability of occurrence of associated earthquakes on PIF determined by Monte Carlo Simulations.

This PTHA study depends on the fully characteristic fault model and the main purpose is to perform PTHA for selected test site. Tuzla test site is one of the coastal districts of Istanbul and located on the southernmost part of the city (Fig 2). The region includes several residential areas but the most critical point about the region is that Tuzla has the biggest shipyard area not 115 only in the Marmara Sea but also in Turkey (Fig 3). In this study we mainly focused on this region because it is about 20km away from the PIF and therefore has high risk of both earthquake and tsunami damage.

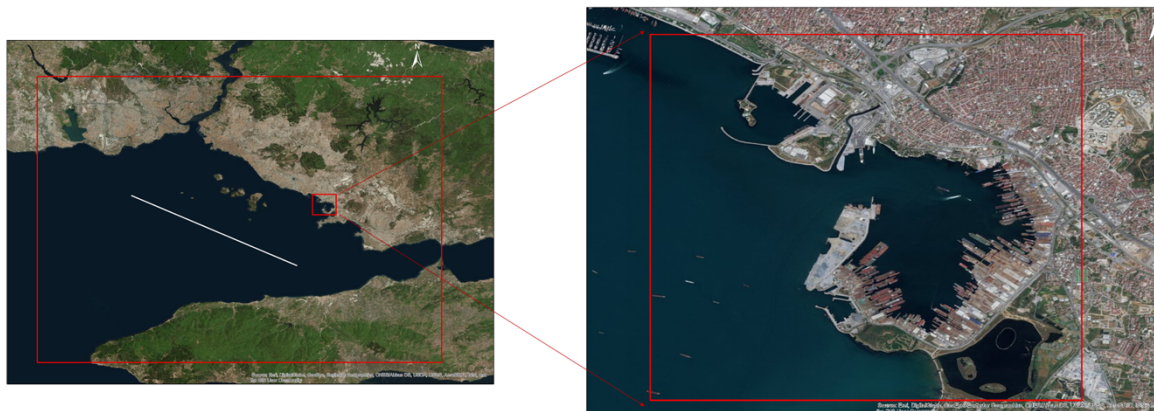
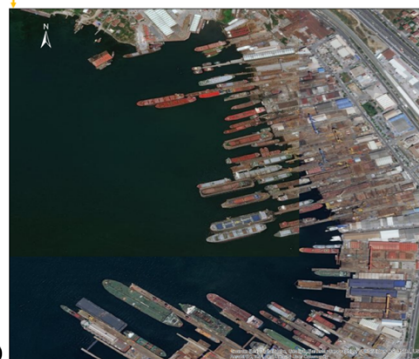
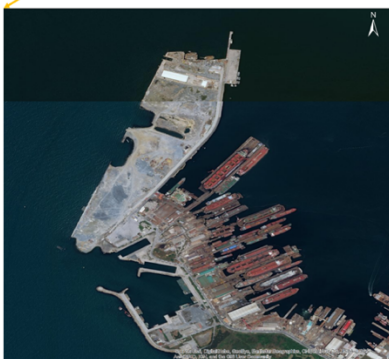


Figure 2: The Marmara Sea Region, Tuzla Test Site and the Location of Prince Islands Fault Segment which is used in the analysis like a straight line (created using ArcMap Version 10.5).



120

Figure 3: Some Important Locations at Tuzla Domain (a) Northern part of the Tuzla domain. (b) Southern part of the Tuzla Domain. (c) Tuzla Shipyard (created using ArcMap Version 10.5).



2 Probabilistic Analysis

Probabilistic tsunami hazard analysis (PTHA), as becoming recently a widely used procedure for coastal zones, is performed
125 for Tuzla region, Istanbul. In tsunami research, this method has been applied for various tsunami source, such as earthquakes,
landslide, volcanic activity etc. in various scales, local, regional and global (Grezio et al., 2017). For the earthquake generated
tsunamis, the method generally adapted from seismic hazard assessment methods (González et al., 2009). Such kind of studies
consider the events that generated by co-seismic sea floor displacement (SPTHA), but numerous tsunami simulations are
required to consider all expected combination of seismic sources and this problem can be solve by applying a simplified event
130 tree approach and a two-stage filtering procedure to reduce the number of required source scenarios without decreasing the
quality and accuracy of inundation maps (Lorito et al., 2015). The earthquake source itself is very uncertain and the
investigation of this uncertainty can be done by building an event tree instead of using logic tree and hazard integrals (Selva
et al., 2016). Logic tree approach can be applied to generation of tsunami hazard curves to decrease the uncertainties by
including branches, which are combination of tsunami sources, magnitude distribution of characteristic tsunamigenic
135 earthquakes, their recurrence interval, and tsunami height estimation procedure based on a numerical simulation (Annaka et
al., 2007). For regional studies, hazard curves can be generated by empirical analysis using available tsunami run-up data.
However, if such data is not available, Monte Carlo simulations, a computational based method widely used in PSHA, should
be considered as a primarily method to generate tsunami hazard curves (Geist and Parsons, 2006; Horspool et al., 2014).
Submarine landslides, on the other hand, are the major tsunami source for passive margins and they have been included in
140 PTHA methodologies (Geist and Lynett, 2014). Probabilistic studies are also applied to develop multi – hazard loss estimation
methodology for coastal regions that exposed to cascading shaking-tsunami hazards due to offshore mega-thrust subduction
earthquakes (Goda and Risi, 2018).

In this study, characteristic earthquake model is used to estimate the earthquake recurrence on PIF. Paleoseismologic studies
suggest that an individual fault tends to generate characteristic earthquakes having a very narrow range of magnitudes. These
145 individual faults have a different frequency distribution than the log linear Gutenberg-Richter frequency-magnitude
relationship (Aki, 1984; Schwartz and Coppersmith, 1984; Youngs and Coppersmith, 1985). According to Aki (1984),
constancy of barriers to rupture through repeated seismic cycles.

PIF is fully characteristic and a characteristic earthquake will rupture entire fault as a whole and release the entire energy.
Therefore, while performing Monte Carlo simulations, area of the fault and fault parameters (strike, dip and rake angles) are
150 used as constant referring to the outcomes of EU 7th Frame Project MARSITE (Ozer Sozdinler et al., 2019). One of the work
package of this project aimed to define the geometry of the possible tsunamigenic faults in the Marmara Sea and 30 different
earthquake scenarios with the different rupture combinations of 32 possible fault segments. Based on these 30 different
earthquake scenarios, tsunami numerical modelling is performed. The definition of fault segments depends on extensive review
of the literature (Alpar and Yaltrak, 2002; Altinok and Alpar, 2006; Armijo et al., 2005; Ergintav et al., 2014; Gasperini et al.,
155 2011; Hebert et al., 2005; Hergert et al., 2011; Hergert and Heidbach, 2010; Imren et al., 2001; Kaneko, 2009; Le Pichon et



al., 2001; Le Pichon et al., 2003; Le Pichon et al., 2014; Oglesby and Mai, 2012; Sengor et al., 2014; Tinti et al., 2006; Utkucu et al., 2009). As a result of this review, each fault segments defined as a rectangular area with hypothetical uniform slip. According to the results of the project, the fault parameters of the PIF, as given in Table 1. The 3D Fault configuration given by the Armijo et al., 2002, which explains fault segmentation in the region depending on morphology, geology and long-term displacement fields, is also fits with the PIF parameters that are used in the project. These parameters are used as constant in this study while assessing probability of occurrence of each earthquake to allow entire fault rupture at different depths with different magnitudes.

Fault Length (km)	Fault Width (km)	Strike	Dip	Rake
33.5	14	119	80	210

Table 1: The area and the focal mechanism of the PIF zone. These are the constant parameters during the Monte Carlo simulation application.

Monte Carlo simulation technique is generally applied to generate earthquake catalogue of a given length of time. In this technique, a list of earthquakes is generated using the frequency - magnitude relationship for each seismic source (Zolfaghari, 2015). Seismic zonation should be done by considering regions that have relatively homogeneous earthquake activity and faulting regimes (Sørensen et al., 2012). After that, tsunami numerical modelling is performed for each event of this synthetic catalogue and tsunami hydrodynamic parameters, mainly maximum wave heights, inundation depth, current velocities, as well as tsunami inundation zones are estimated. Regional PTHA studies can be used as a guide for further local studies to develop of a more effective tsunami warning systems. Tsunami risk assessment will serve the best for the needs of societies when associate regional studies with the local ones (Sørensen et al., 2012).

Monte Carlo simulation technique allows generating a list of earthquakes based on a frequency-magnitude relationship. This technique depends on a uniformly distributed source model and it provides equal chance to each earthquake source. As a result, synthetic earthquake catalogue will have uniformly random distributed earthquake sources (Zolfaghari, 2015).

Using Monte Carlo simulation, a synthetic earthquake catalogue is generated by selecting earthquake magnitude and depth randomly and using area and directivity of the fault as a constant (Table 1). We performed Monte Carlo simulations 100 times for to having 100 different earthquake scenarios. The number of earthquakes in the catalog is selected as a reasonable number, which represents the number of iterations randomly done in MC simulations for having a synthetic earthquake scenario. Since the probabilistic analyses are time-dependent in our study, the catalog duration represented as the number of earthquakes times recurrence period (i.e. 100x250) is not used for PTHA analysis.

Earthquake magnitude is one of the parameters randomly selected by the Monte Carlo technique. Based on a characteristic earthquake model, individual faults tend to rupture entire fault when a large earthquake occurred. This model assumes that



characteristic earthquake releases all of the seismic energy during the fault rupture and the magnitude of the earthquake depends on the dimension of fault (Abrahamson and Bommer, 2005).

As mentioned previously, only the Prince Islands fault is considered as earthquake source with approximately 34 km in length and 14 km in width (Ozer Sozdinler et al., 2019; Karabulut et al., 2002). This fault zone is assumed that it has potential to generate a characteristic earthquake and according to Wells and Coppersmith (1994) scaling relation between fault area and magnitude (Eq. 1), this fault can generate a characteristic earthquake with the magnitude varying between Mw 6.5-7.1.

$$Mw = a + b * \log(L * W) \quad (1)$$

In this equation, a and b are coefficient and standard errors, which are 4.33 and 0.09 with standard deviations 0.12 and 0.05 respectively, L is fault length and W is the fault width.

Displacement on the fault surface calculations are done, for each randomly selected magnitude, using the formulation of Aki (1966),

$$D = \frac{Mo}{\mu A} = \frac{10^{(Mw+6.07)*1.5}}{\mu A} \quad (2)$$

where D is displacement on the fault surface, Mw is moment magnitude, μ is the shear modulus ($\mu=30$ GPa), and A is the fault area.

Seismogenic thickness and the location of the earthquake is another important parameter required for earthquake and tsunami source. At first, the Prince Islands fault zone is accepted as fully characteristic and an earthquake should rupture the entire fault area. Therefore, it is assumed that if the rupture starts at the center of the fault and continues in both directions, the fault will rupture entirely. For this reason, the locations of the earthquakes are accepted as the midpoint of Prince Islands fault zone for each earthquake scenarios (Ozer Sozdinler et al., 2019).

For the seismogenic thickness, the seismic activity of the northern segment of NAFZ starts at the depth of 5 km (Karabulut et al., 2003). The bottom of the seismogenic thickness can be determined based on the after-shock activity of the 17 August 1999 Izmit Earthquake. The earthquakes on the northern scarp of the Çınarcık basin are observed between the depths of 5 and 14 km. The mechanism of events between the depth of 5 and 10 km shows the behavior of normal faulting. On the other hand, strike-slip mechanism dominates the depths below 10 km to 14 km. As a result, seismic activity can be observed between the depths of 5-14 km and fault plane solutions show normal and strike-slip mechanisms in this area (Karabulut et al., 2002).

2.1 Probability Calculations

This section is describing the details of various methods, models and assumptions considered for performing the probability calculations before correlating these results with the tsunami wave heights calculated by numerical modeling. In time-independent earthquake occurrence models, probability of an event occurrence follows a Poisson distribution in a given certain period of time. Therefore, the result of this model does not vary in time. However, probability of an earthquake occurrence based on the time that was passed since the occurrence of last event and it follows a Brownian passage time (BPT), log-normal or another probability distribution. In this model, variability of the frequency of events and the elapsed time from the last



characteristic event are the additional required information in addition to the recurrence time of earthquake and the probability
220 of an event occurrence increases with the elapsed time. (Cramer et al., 2000; Petersen et al., 2007).

Calculation of probability in multi – segment ruptures and more complicated models includes Gutenberg Richter magnitude
– frequency relationship (Gutenberg and Richter, 1944). The application of time – dependent models based on characteristic
earthquake model which assumes all large events occurring along a particular fault segment would have similar magnitudes,
rupture area and average displacements (Schwartz and Coppersmith, 1984).

225 It should be noted that, in this study, PIF is considered as the only source for the earthquake and tsunami. Time dependent
probabilistic model is followed for the probability calculations; because, instead of using multi – segment rupture scenarios,
only one fault is considered.

Historical records show that, PIF generates an earthquake with the recurrence interval of about 250 years and the latest event
occurred in 1766 (Ambraseys, 2002). However, this event caused the rupture of 58 km-long northern part of NAFZ from Izmit
230 to Tekirdağ (Ambraseys and Finkel, 1995; Ambraseys and Jackson, 2000). The earthquake that occurred on 2 September 1754
is the latest characteristic event for the Prince Islands segment and it caused the rupture of a 36 km long fault segment
(Ambraseys and Jackson, 2000).

In the time-dependent approach, Brownian passage time (BPT) probability model is used to obtain the recurrence time
probability of the earthquake in the fault segment. This model does not show significant difference with the log – normal
235 distribution except for consideration of very long elapsed times from the last characteristic event (Petersen et al., 2007). An
earthquake releases all energy loaded on the fault and then starts the new failure cycle. The time interval between consecutive
earthquakes shows a Brownian passage time distribution and that can be useful to forecast long term seismic events by
generating a time – dependent model (Matthews et al., 2002). The Working Group on California Earthquake Probabilities
(1999) and the Earthquake Research Committee (2001) have already implemented this time – dependent approach to the San
240 Francisco Bay and Japan, respectively, for the prediction of long-term events (Petersen et al., 2007). This model depends on
the time period passed since the last characteristic event and recurrence time of the earthquake. The probability density function
for BPT model (Matthews et al., 2002) is given by,

$$f(t, Tr, \alpha) = \left(\frac{Tr}{2\pi\alpha^2 t^3}\right)^{1/2} \exp\left(\frac{(t-Tr)^{1/2}}{2Tr\alpha^2 t}\right) \quad (3)$$

where t is the elapsed time from the last characteristic event and α is the aperiodicity (also known as the coefficient of
245 variation). Aperiodicity defines the regularity of the expected characteristic earthquakes on the fault and varies between the
0.3 and 0.7. This parameter, which is known as the parameter defining how much an expected characteristic earthquake occurs
regularly or irregularly on any fault segment (Murru et al., 2016), was taken as 0.5 in this study (Parsons, 2004). The mean
recurrence interval of earthquakes (Tr) can be defined as the ratio between the mean moment of repeating earthquakes (seismic
moment) and the long-term moment accumulation rate on the fault (moment rate). Seismic moment can be obtained using the
250 formulation of Kanamori (2004) and the moment rate of the fault is calculated from fault area and long-term slip rate of the
fault (WGCEP 2003).



$$Tr = \frac{Mo}{\dot{M}o} = \frac{10^{(Mw+6.07)*1.5}}{\mu VA} \quad (4)$$

In this equation, M_w is moment magnitude, μ is the shear modulus, V is long-term slip rate in mm/yr and A is the fault area. The moment magnitude value in Eq. (4) was selected randomly using Monte Carlo simulations. Thus, seismic moment (M_o) and the mean recurrence time (Tr) were calculated for each earthquake scenario. Long term slip rate is also selected as 17 mm/yr for this equation (Ergintav et al., 2014).

Probability of the earthquake occurrence on the fault is calculated based on the probability density function approach. The probability of occurrence of an event in the next ΔT years, given that it has not occurred in the last t years is given by (Erdik et al., 2004),

$$P(t, \Delta T) = \frac{\int_t^{t+\Delta T} f(t)dt}{\int_t^{t+\infty} f(t)dt} \quad (5)$$

In this case, probability of a characteristic earthquake was calculated using ΔT as 50 and 100 years.

3 Tsunami Numerical Modelling

Tsunami simulations are performed for each earthquake in synthetic catalogue using tsunami numerical model NAMI DANCE (NAMI DANCE, 2011). The code is the user-friendly version of TUNAMI-N2 (Imamura et al., 2001) developed in C++ language, which computes all fundamental parameters of tsunami motion in shallow water and in the inundation zone. It uses explicit numerical solution of shallow water wave equations with finite-difference technique and allows for better understanding of the effect of the tsunami waves (Shuto et al., 1990; Imamura, 1989). NAMI DANCE can solve both Linear and Nonlinear Shallow Water (NSW) Equations with selected coordinate system (Cartesian or spherical) and calculates the tsunami motion. NSW equations are preferable in deep water because of reasonable computer time and memory and calculates the results in acceptable error limit (Insel, 2009). NAMI DANCE is validated and verified using NOAA standards and criteria for tsunami currents and inundation (Synolakis et al., 2007; Synolakis et al., 2008). The numerical solutions of NAMI DANCE are also tested, validated and verified against analytical solutions, laboratory measurements and field observations (NTHMP, 2015; Lynett et al., 2017; Velioglu, 2009)

NAMI DANCE calculates tsunami generation using Okada (1985) equations. In this study, water surface distribution of tsunami source (initial wave amplitude) are calculated with this method for 100 earthquakes of the synthetic earthquake catalogue prepared by Monte Carlo simulations.

Before starting tsunami simulations, the necessary inputs should be prepared precisely in order to obtain reliable results. Bathymetry - topography data is one of the most important input in NAMI DANCE that significantly effects the reliability of results especially in shallow water zone due to the nature of NSW Equations. Therefore, the bathymetry - topography data in the smallest domain includes digitized coastline, and sea and land structures in high resolution with 3m grid size.

Synthetic gauge point file is another required input of the NAMI DANCE. In addition to the calculation of principal tsunami hydrodynamic parameters, program can also calculate the change of water level, current velocity and flow depth over time in



every gauge point. Therefore, various gauge points are selected along the coast of nested domains, near shore and offshore and close to some critical structures on land.

285 During the inundation of tsunami waves, current velocity is an important tsunami parameter in land and sea, especially in ports and bays. Strong current velocities may cause dragging offshore or landing of sea vessels inland. This parameter as well as tsunami wave amplitude, inundation depth and Froude number can be calculated by NAMI DANCE. However, in this study, the results are represented based on only the probability of exceedance of threshold values for water surface elevation and inundation depth.

290 NAMI DANCE can make nested analyses under the condition that grid size of study domains have a certain 1:3 ratio between each other. Therefore, we generated four nested domains having the coarsest grid size as 81 m and the finest grid size as 3 m with 1:3 ratio in GIS environment. Coarser data includes multi-beam bathymetric measurements and 900m grid sized GEBCO data in the sea and 30m grid sized ASTER data on land. Coastline, and sea and land structures are also digitized in GIS environment and included in 3m grid sized high resolution bathymetry - topography data in the smallest domain (Fig 4).



295

Figure 4: Nested domains for tsunami numerical modelling. Red rectangles show the limits of these domains. Grid size of these domains have a certain 1:3 ratio between each other (created using ArcMap Version 10.5).

4 Results and Discussion

300 In this study, tsunami hydrodynamic parameters are calculated in both coarsest domain (whole Marmara Sea) and finest domain (Tuzla region). The main parameters focused in this study are the tsunami wave heights and inundation depths and the results are shown in the terms of probability of exceedance of threshold wave height and inundation depth values within the next 50 and 100. The situation for the next 500 years is not considered because the return period of the fault rupture is about 250 years



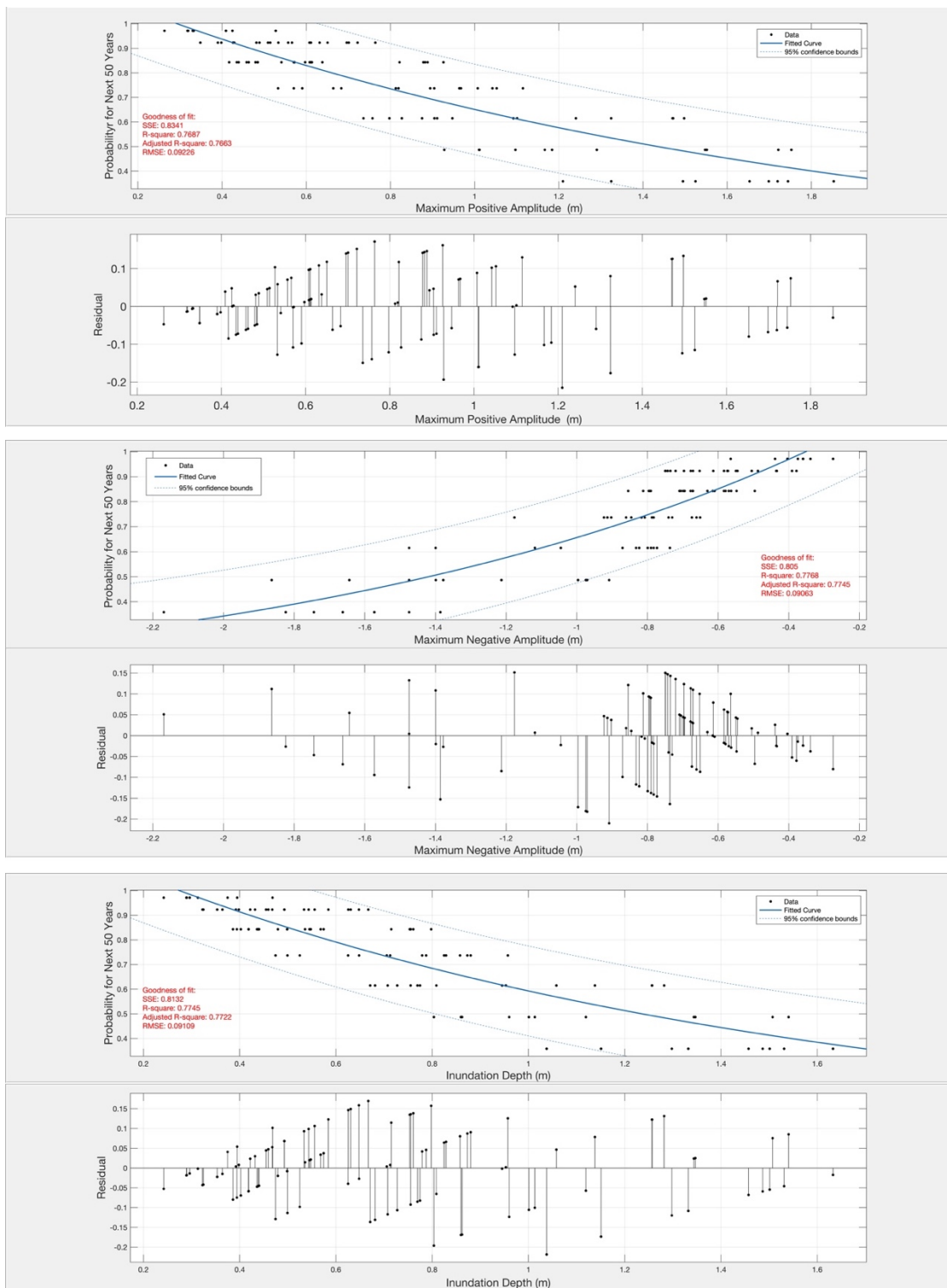
305 which means this fault generates at least one earthquake within the next 500 years. In other words, probability of exceedance for the next 500 years will be about 99%.

We present the results of the PTHA for Tuzla test site in terms of three different visualization categories for the next 50 and 100 years. First, graphics are prepared to show general distribution of probability of occurrence with respect to considered tsunami hydrodynamic parameters, which are minimum and maximum water surface elevation and inundation depth. Second, tsunami inundation maps that show probability of exceedance of 0.3 m inundation depth for different time periods are generated for Tuzla region in order to observe flooded areas and their probabilities clearly. And finally, the probability map of exceedance of 0.3 m wave heights at synthetic gauge points are represented as bar charts.

4.1 Graphs of Probability of Exceedance for Entire Synthetic Earthquake Catalogue

The graphics are generated to demonstrate the probabilities of occurrences corresponding to the minimum and maximum water surface elevations and inundation depth calculated from tsunami sources of each earthquake in synthetic earthquake catalogue. It should be noted that in case of having same magnitude of earthquakes in two different earthquake scenario of the catalogue, the probability of occurrences of these scenarios would be the same. However, since they would have different focal depths the tsunami initial wave height calculated by Okada (1985) will be different which results the calculation of different hydrodynamic parameters. As a result, the graphs show different maximum water surface elevations having the same probability of occurrences.

320 In Figure 5, graphics of probabilities of occurrences according to maximum and minimum water surface elevation (maximum water withdraw) and inundation depth for next 50 years are represented, respectively. According to these graphs, tsunami wave heights up to 1 m and withdrawal of the waves around 1 m have approximately 65% probability of occurrence. Tuzla region includes various shipyards, ports and other important facilities. Therefore, probability of the withdrawal of the water is important as much as of maximum water surface elevation. 1 m height of wave withdrawal may cause the ships to be stranded at the ports and results extreme financial losses. The probability for having 1 m inundation depth, on the other hand, can be predicted as about 60%.

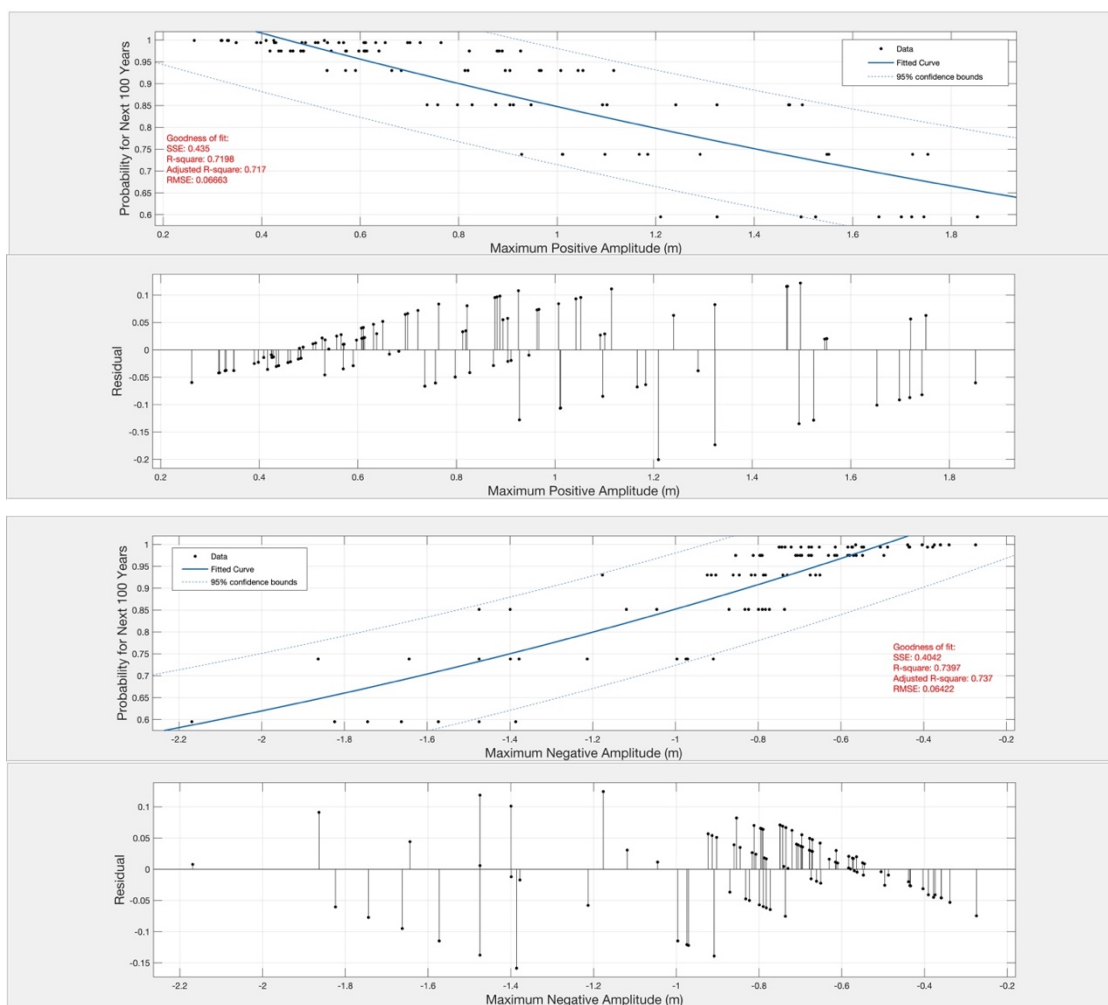


330 **Figure 5: Probabilities of Exceedance Corresponding to Maximum Water Surface Elevation, Minimum Water Surface**



Elevation and Inundation Depth for the next 50 years. Black dots represent the probability of exceedance of tsunami hydrodynamic parameter for each event in the catalog. Blue line is the best fit curve to the data and dashed blue line is the 95% confidence boundary of fitted curve. Residual of the fit is represented for each probability curves.

335 The situation for next 100-years (Fig 6) obviously shows that probability of occurrences would increase with the time. The probability of exceedance of 1 m water surface elevation and 1 m wave withdraw reaches up to 85%. Probability of exceedance of inundation depth also changes significantly. The probability of exceedance of 1 m inundation depth is found around 80% from the graphics.



340

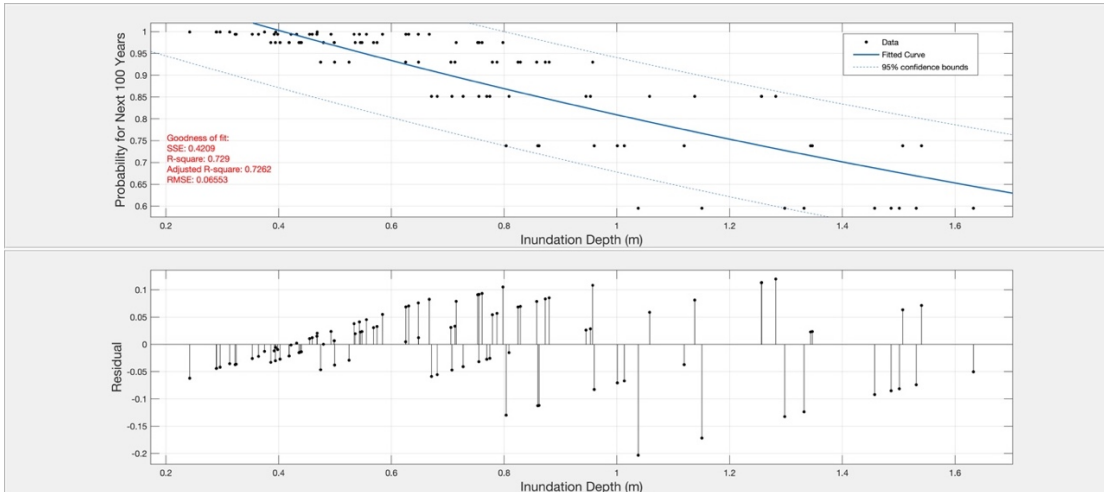


Figure 6: Probabilities of Exceedance Corresponding to Maximum Water Surface Elevation, Minimum Water Surface Elevation and Inundation Depth for the next 100 years. Black dots represent the probability of exceedance of tsunami hydrodynamic parameter for each event in the catalog. Blue line is the best fit curve to the data and dashed blue line is the 95% confidence boundary of fitted curve. Residual of the fit is represented for each probability curves.

Considering the results of the whole simulations, maximum water surface elevation, minimum water surface elevation (maximum withdraw) and inundation depth are calculated in worst case earthquake scenario as 1.85 m, 2.16 m and 4.48 m respectively. The probabilities of occurrence of these values are 35% for next 50 years and 60% for next 100 years.

350 4.2 Probabilistic Tsunami Inundation Maps for Tuzla Test Site

Inundation maps of Tuzla domain are also prepared for the next 50 and 100-years in GIS environment. Even if inundation depth is in the order of few centimeters, it can lead to dragging of people in coastal regions due to the high current velocities of the waves. Therefore, these inundation maps have a great significance to understand the flooded areas in study domain and the amount of penetrated water inland.

355 Generation of inundation maps are based on the probability of exceedance of 0.3 m inundation depth. There are several studies in literature proving both experimentally and numerically that tsunami waves with the order of 0.3 m height have a potential to collapse a human body (Jonkman and Penning-Rowse, 2008; Takagi et al., 2016). For this reason, only the earthquake scenarios that generated inundation depths larger than or equal to 0.3 m threshold value are considered. Inundation depth files, which is one of the outputs of the NAMI DANCE, are used and the inundation depth values calculated as spatial distribution of maximum inundation depths at each grid node are replaced with the probability of occurrence of the respective earthquake scenario. As a result, we obtained the plots showing the probability of occurrence of inundation depths calculated higher than 0.3m in inundated zone for an earthquake scenario in the catalog. This procedure is repeated for all 100 earthquake scenarios. 360 After that, the mean (average) inundation depth values are calculated at each grid node and thus the spatial distribution of probability of exceedance of 0.3 m inundation depth in inundation zone is obtained for a specific time interval (Fig 7).



365 Figure 7 shows the inundation maps of Tuzla shipyard for the next 50 and 100-years. Most of the area in Tuzla shipyard region have probability of exceedance between 10% and 20% for both of the next 50 and 100 years. However, some places in the northern and southern part of the area and inside the bay show larger than 75% probability of inundation within the next 100 years. Maximum inundation distance is observed as around 60 m in the test site.





370

Figure 7: Probabilistic Tsunami Inundation Maps for Tuzla Study Domain representing the Probability of Exceedance of 0.3 m Inundation Depth within the Next 50 and 100 Years. Change of colors from green to red represents the increasing of probability of exceedance (created using ArcMap Version 10.5).

375 In Figure 8, probabilistic inundation maps of one of the most important facilities in study region are represented for the next 50 and 100 years. The area has high potential to expose tsunami waves with probability larger than 50% for the next 50 years. In 100 years, this probability increases and varies between 75% and 90%. No significant inundation zone is observed along the coast of the seawall and the peninsula. This may be due to the high ground elevation of these zones. Tsunami waves are inundated up to 45 m inside the small bay. This inundation distance could cause severe damage to shipyard and other constructions if corresponding current velocities are also significant.



380



Figure 8: Probabilistic Tsunami Inundation Maps of Northern Part of Tuzla Study Domain representing the Probability of Exceedance of 0.3 m Inundation Depth for the Next 50 and 100 Years. Change of colors from green to red represents the increasing of probability of exceedance (created using ArcMap Version 10.5).

385 In the next figure (9), the southern part of the Tuzla shipyard is seen according to probabilities of inundation for the next 50 and 100 years. Very limited area in the coastal zone is inundated with the probability between 30% and 50% within the next 50 years. The probability reduces up to 10% at some inner locations from the coastline. For 100-year recurrence time, the situation is almost the same. Only minor parts of the region at the south approaches up to 75% - 90% probability of exceedance of 0.3 m inundation depth threshold. The maximum inundation distance is calculated about 60 m. The inundated region does not include any important facility or structure and the effect of the tsunami will be minimal. The inundation distance decreases to 10 m at the other parts of the region.

390





395 **Figure 9: Probabilistic Tsunami Inundation Maps for the Southern Part of Tuzla Study Domain representing the Probability of Exceedance of 0.3 m Inundation Depth for the Next 50 and 100 Years. Change of colors from green to red represents the increasing of probability of exceedance (created using ArcMap Version 10.5).**

400 The region indicated in Fig 10 is located inside the bay and includes a large part of the shipyard area. This area includes lots of large and small piers and ship construction facilities. The situation is more or less the same with the previous region (Fig 8). Probability of having larger than 0.3 m inundation depth changes between 30% and 50% within the next 50 years, while only a few places show 75% - 90% probability for the next 100 years along the coast. Moreover, maximum inundation distance is calculated as 25 m for this zone. Even if the probability of inundation is low, these zones should be taken into consideration before constructing a new structure.





Figure 10: Probabilistic Tsunami Inundation Maps of Shipyard Area in Tuzla Study Domain representing the Probability of Exceedance of 0.3 m Inundation Depth for the Next 50 and 100 Years. Change of colors from green to red represents the increasing of probability of exceedance (created using ArcMap Version 10.5).

410

4.3 Synthetic Gauge Points

Finally, the probability of exceedance of 0.3 m wave heights at synthetic gauge points are presented by bar charts to consider the near shore effect of tsunami waves along the western coast of Istanbul. Because of the closeness to the fault zone, the southeast coasts of the city are under the threat of the significant tsunami damage. Similar with the method applied during the preparation on probabilistic inundation maps, the earthquake scenarios with wave heights at synthetic gauge points larger than or equal to 0.3 m are selected and replaced with the probability of each scenario according to wave heights and after that the average probabilities at each synthetic gauge point are obtained accordingly.

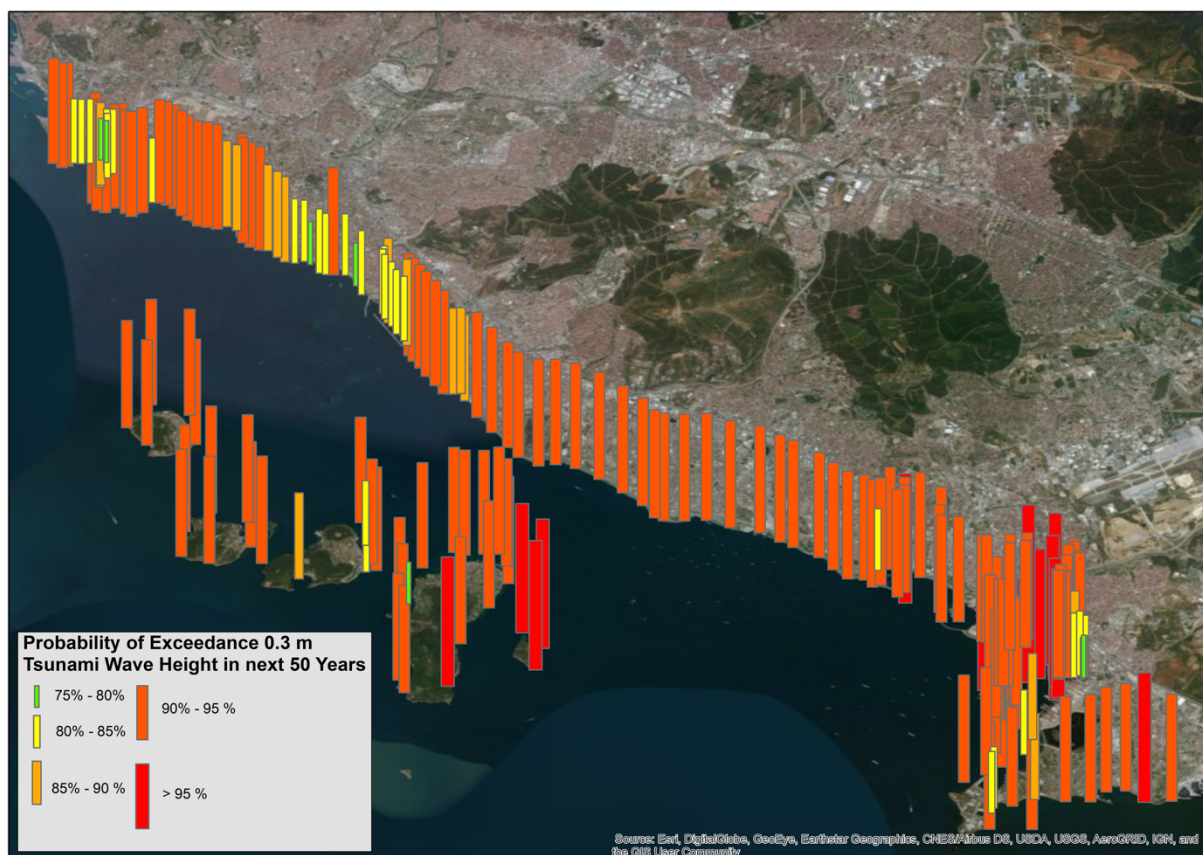
Figure 11 demonstrates the probability of exceedance of 0.3m wave height at synthetic gauge points along the western coast of the Istanbul within the next 50 and 100 years. The probability is increasing while color scale changes from green to red. According to this figure, minimum probability of exceedance is shown as 75% at some points. Except for a few of 228 synthetic gauge points, all points have larger than 90% probability of exceedance of 0.3 m wave height within the next 50-years time

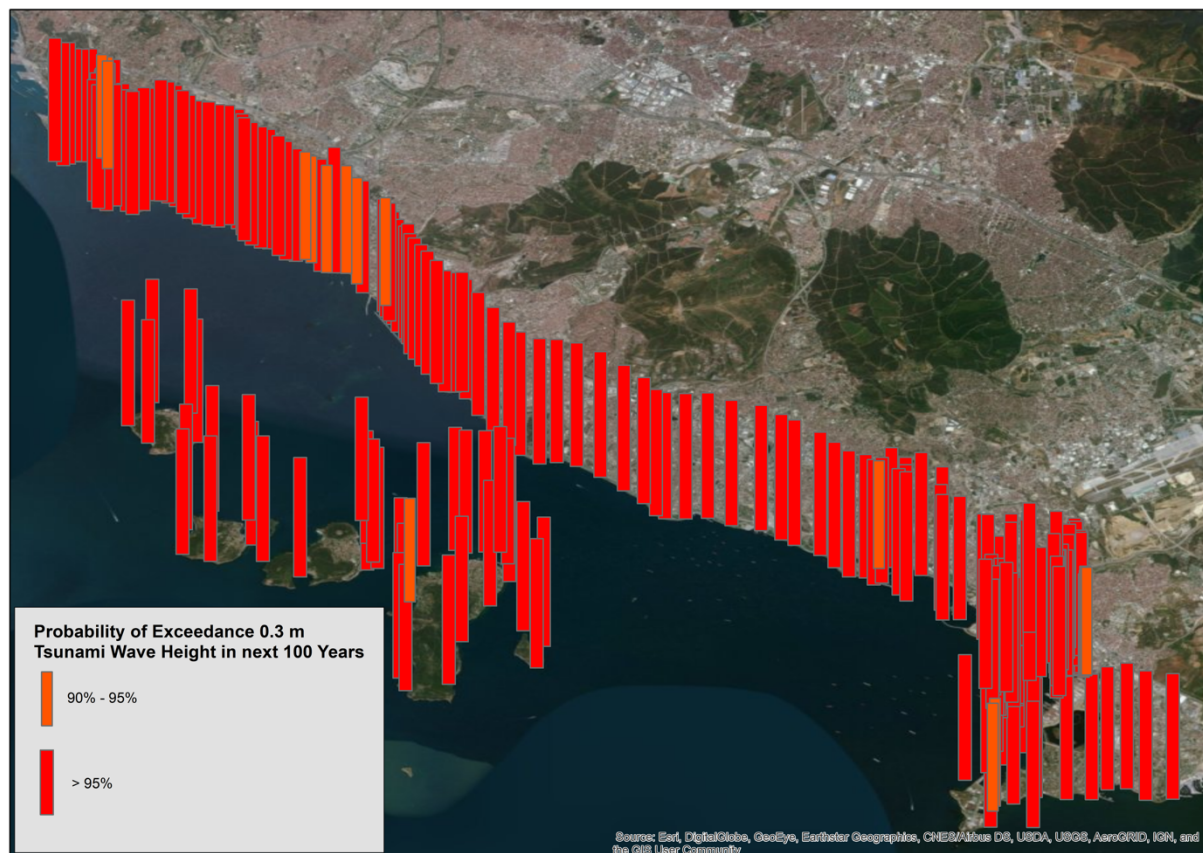
420



scale.

This condition is very serious since there are so many residential areas and important spots such as ports and recreational facilities in this region. The minimum probability of occurrence, which can generate tsunami waves with at least 0.3 m wave heights, reaches up to 90% for the next 100-year time period. However, 95% probability of exceedance of 0.3 m wave height dominates the region for this time scale.





430 **Figure 11: Probability of Exceedance of 0.3 m Tsunami Wave Height within the next 50 and 100 years at Synthetic Gauge Points**
(yellow rectangles show the Tuzla study domain, change of colors from red to green on the bars represents the decreasing of
probability of exceedance (created using ArcMap Version 10.5).

4.4 Uncertainties

PTHA studies includes some uncertainties because of the rare occurrence nature of the large events. Quantification of these
435 uncertainties generally includes mixture of empirical analyses and subjective judgment.

Uncertainties of PTHA can be divided into two; as aleatory and epistemic variability. Aleatoric uncertainty is the natural
randomness of the physical process. The aleatory variable effects the results because it is incorporated directly into the hazard
calculations (Abrahamson and Bommer, 2005). Adding data does not help to decrease the uncertainty. However, knowledge
about the process may decrease this unpredictability.

440 Epistemic uncertainty is the lack of knowledge and data. Accurate probability distributions of input cannot be known. For
example, assuming that probability of occurrence of an event follows Poisson distribution. However, return periods of events
do not simply fit to this distribution (Gonzalez et al., 2013). Unlike aleatoric one, epistemic uncertainty can be decreased when
more information is available (Godinho, 2007). Different techniques, such as logic tree, Bayesian method etc., have been



developed to reduce these uncertainties.

445 In this study, the return period of rupture of PIF is assumed as 250 years referring to previous scientific studies and probabilistic model is established based on the characteristic fault model of PIF. Those studies naturally include uncertainties which are naturally reflected to this PTHA study. Besides, MC simulation itself also includes uncertainty as being performed hundred times to create synthetic earthquake scenarios. The effect of uncertainty in aperiodicity parameter is also existing and can be reduced by including different parameters to MC simulation. Therefore, the tsunami hydrodynamic parameters associated with
450 the probability of occurrence of the corresponding scenario preserve the same uncertainty.

5 Conclusion

In this study, time-dependent PTHA is performed in Tuzla region, Istanbul for the purpose of understanding the probability of having tsunami inundation after the Prince Islands fault rupture. The study combines tsunami numerical modelling with probabilistic approach, which is modified from probabilistic seismic hazard analysis. Probability calculations have been done
455 based on the time-dependent BPT model, which depends on the time period passed since the last characteristic event and the recurrence time of earthquake. After that, synthetic earthquake catalogue is generated using Monte Carlo simulation technique and tsunami numerical modelling was performed depending on this earthquake catalogue using NAMI DANCE code in GPU environment.

460 Results of the numerical modelling was demonstrated in three different ways for the next 50 and 100 years. The first one was the graphs showing the change of probability with the maximum and minimum water surface elevation and inundation depth for different time intervals. Second type of demonstration of results was the probabilistic tsunami inundation maps for Tuzla region. Finally, the probability maps of exceedance of 0.3 m wave heights at synthetic gauge points are represented as final outcomes.

465 The main results of this study can be summarized as follows:

- According to the distribution of probability with respect to tsunami hydrodynamic parameters, the probability of exceedance of 1 m maximum positive and negative water surface elevation is 65% within next 50 years. The probability decreases for 1 m inundation depth up to 60%.
- Considering probabilities for next 100 years, 85% probability of exceedance of 1 m was calculated. For 1 m inundation depth, probability of exceedance is obtained about 80%.
- As a result of whole simulations, 1.85 m, -2.16 m and 4.48 m were calculated for maximum and minimum water surface elevation and inundation depth, respectively with the probability of 35% for the next 50 years, 60% for next 100 years.
- Inundation maps, indicate that inundation of tsunami waves that are equal to or larger than 0.3 m have probability mostly higher than 10 % and 20% for the next 50 years and 100 years, respectively. The probability of occurrence of 0.3m inundation depth was calculated as maximum 75% for the next 100 years. Maximum inundation distance is calculated as 60 m and observed in the southern part of the finest 3m grid-sized study area.
- Probabilistic results for the exceedance of 0.3 m wave height at synthetic gauge points demonstrate that only few of them has a probability between 75% - 85%, however several points have more than 90% probability for the next 50
475 years. Probability of exceedance increases by more than 95% for the next 100-years.

480 The tsunami impact of the Prince Islands fault rupture along the Tuzla coast is very important as proposed with the results of this study. However, as further steps of this study, PTHA can be done for the other critical test sites along the Marmara Sea



that are close to the PIF segment. Besides, it is also advantageous to consider the other fault segments, their various rupture combinations and complex rupture probabilities in Marmara Sea as further studies. Previously in the framework of the MARSite project, tsunami arrival times and maximum wave amplitudes are calculated along the coast of the Marmara Sea using different earthquake scenarios and a tsunami scenario database was obtained in deterministic approach (Ozer Sozdinler et al., 2019). Results of this study show that, arrival time of tsunami waves is very short in Marmara Sea for most of the scenarios which complicates the tsunami early warning operations and evacuation actions. However, due to the short arrival times of first tsunami wave along Marmara coast, the tsunami inundation scenario databases would be of great importance in such conditions. It would be the best option for the decision makers and civil protection authorities to have the inundation maps prepared also in probabilistic approach in order to realize the possibility of exceedance of selected threshold inundation depth for certain critical coastal locations.

This study shows a methodology for PTHA with time – dependent probabilistic model using only one fault (PIF) as earthquake and tsunami source. Furthermore, this study can be developed including some connected faults to the PIF in both time – dependent and time - independent probability calculations and Brownian passage time (BPT) probability can be combined with static Coulomb stress changes on the faults. Brownian passage time (BPT) model can also be improved by including different aperiodicity parameters. The probability of occurrence of earthquakes is the main focus of this study to perform tsunami hazard analyses. However, submarine landslides are other critical important sources for tsunami generation in Marmara Sea. Probabilities of sliding areas and the sliding volumes can be considered in the analyses. Submarine landslide generated tsunamis can be coupled with the earthquake triggered tsunamis in order to obtain integrated PTHA in the Marmara Sea.

Acknowledgements

The authors would like to acknowledge the project MARSite - New Directions in Seismic Hazard assessment through Focused Earth Observation in the Marmara Supersite (FP7-ENV.2012 6.4-2, Grant 308417) and SATREPS Project MaRDIM (Earthquake and Tsunami Disaster Mitigation in the Marmara Region and Disaster Education in Turkey). The authors would like to especially thank Prof. Dr. Ahmet Cevdet Yalçiner for his valuable feedback and effort during this study and great support of Bora Yalçiner and Andrey Zaitsev in the development and improvement of the NAMI DANCE numerical code. We also would like to thank Dr. Öcal Necmioğlu, Dr. Maura Murru, Dr. Giuseppe Falcone, Prof. Dr. Semih Ergintav, Prof. Dr. Sinan Akkar, Dr. Mine Demircioğlu and Prof. Dr. Mustafa Erdik for their valuable support and feedback. The Generic Mapping Tools (GMT; Wessel and Smith, 1998) was used for plotting tectonic map of Turkey and bathymetric map of Marmara fault system. Other maps throughout this paper were created using ArcGIS® software by Esri. ArcGIS® and ArcMap™ are the intellectual property of Esri and are used herein under license. Copyright © Esri. All rights reserved. For more information about Esri® software, please visit www.esri.com.



References

- 515 Abrahamson, N. A., and Bommer, J. J.: Probability and uncertainty in seismic hazard analysis, *Earthquake spectra* 21(2), 603-607, <https://doi.org/10.1193/1.1899158>, 2005.
- Aki, K.: Generation and propagation of G waves from the Niigata Earthquake of June 16 1964. Part 2. Estimation of earthquake movement, released energy, and stress-strain drop from the G wave spectrum, *Bull. Earthq. Res. Inst.*, 44, 73-88, <https://ci.nii.ac.jp/naid/10006221613/en/>, 1966.
- 520 Aksu, A. E., Calon, T. J., Hiscott, R. N., and Yasar, D.: Anatomy of the North Anatolian Fault Zone in the Marmara Sea, Western Turkey: extensional basins above a continental transform, *Gsa Today* 10(6), 3-7, 2000.
- Altinok, Y., Alpar, B., Özer, N., and Aykurt, H.: Revision of the tsunami catalogue affecting Turkish coasts and surrounding regions, *Nat. Hazards Earth Syst. Sci.*, 11, 273-291, <https://doi.org/10.5194/nhess-11-273-2011>, 2011.
- Ambraseys, N. N. N., and Finkel, C. F.: Seismicity of Turkey and Adjacent Areas: A Historical Review 1500-1800, MS Eren, 1995.
- 525 Ambraseys, N. N., and Jackson, J. A.: Seismicity of the Sea of Marmara (Turkey) since 1500, *Geophysical Journal International* 141(3), F1-F6, <https://doi.org/10.1046/j.1365-246x.2000.00137.x>, 2000.
- Ambraseys, N.: The seismic activity of the Marmara Sea region over the last 2000 years, *Bulletin of the Seismological Society of America*, 92(1) 1-18, <https://doi.org/10.1785/0120000843>, 2002.
- 530 Armijo, R., Meyer, B., Navarro, S., King, G., and Barka, A.: Asymmetric slip partitioning in the Sea of Marmara pull-apart: A clue to propagation processes of the North Anatolian fault?, *Terra Nova* 14(2), 80-86, <https://doi.org/10.1046/j.1365-3121.2002.00397.x>, 2002.
- Armijo, R., Pondard, N., Meyer, B., Uçarkus, G., de Lépinay, B. M., Malavieille, J., ... and Cagatay, N.: Submarine fault scarps in the Sea of Marmara pull-apart (North Anatolian Fault): Implications for seismic hazard in Istanbul, *Geochemistry, Geophysics, Geosystems*, 6(6), <https://doi.org/10.1029/2004GC000896>, 2005.
- 535 Armijo, R., Meyer, B., Hubert, A., and Barka, A.: Westward propagation of the North Anatolian fault into the northern Aegean: Timing and kinematics, *Geology* 27(3) 267-270, [https://doi.org/10.1130/0091-7613\(1999\)027<0267:WPOTNA>2.3.CO;2](https://doi.org/10.1130/0091-7613(1999)027<0267:WPOTNA>2.3.CO;2), 1999.
- Bohnhoff, M., Bulut, F., Dresen, G., Malin, P. E., Eken, T., and Aktar, M.: An earthquake gap south of Istanbul, *Nature communications*, 4 1999, <https://doi.org/10.1038/ncomms2999>, 2013.
- 540 Barka, A.: The 17 august 1999 Izmit earthquake, *Science* 285(5435) 1858-1859, <https://doi.org/10.1126/science.285.5435.1858>, 1999.
- Emre, Ö., Duman, T. Y., Özalp, S., Elmacı, H., Olgun, Ş., and Şaroğlu, F.: Active fault map of Turkey. Special Publication, *Bull Earthquake Eng* (2018) 16: 3229, <https://doi.org/10.1007/s10518-016-0041-2>, 2018.
- 545 Ergintav, S., Reilinger, R. E., Çakmak, R., Floyd, M., Cakir, Z., Doğan, U., ... and Özener, H.: Istanbul's earthquake hot spots: Geodetic constraints on strain accumulation along faults in the Marmara seismic gap, *Geophysical Research Letters*, 41(16), 5783-5788, <https://doi.org/10.1002/2014GL060985>, 2014.
- Erdik, M., Demircioglu, M., Sesetyan, K., Durukal, E., and Siyahi, B.: Earthquake hazard in Marmara region, Turkey, *Soil Dynamics and Earthquake Engineering* 24(8), 605-631, <https://doi.org/10.1016/j.soildyn.2004.04.003>, 2004.
- 550 Flerit, F., Armijo, R., King, G. C. P., Meyer, B., and Barka, A.: Slip partitioning in the Sea of Marmara pull-apart determined from GPS velocity vectors, *Geophysical Journal International* 154(1) 1-7, <https://doi.org/10.1046/j.1365-246X.2003.01899.x>, 2003.
- Flerit, F., Armijo, R., King, G., and Meyer, B.: The mechanical interaction between the propagating North Anatolian Fault and the back-arc extension in the Aegean, *Earth and Planetary Science Letters* 224(3-4), 347-362, <https://doi.org/10.1016/j.epsl.2004.05.028>, 2004
- 555 Geist, E. L., and Parsons, T.: Probabilistic analysis of tsunami hazards, *Natural Hazards*, 37(3) 277-314, <https://doi.org/10.1007/s11069-005-4646-z>, 2006.
- Godinho, J.: Probabilistic Seismic Hazard Analysis an Introduction to Theoretical Basis and Applied Methodology, Mcs. thesis, University of Patras, Greece, 2007.
- 560 González, F. I., Geist, E. L., Jaffe, B., Kânoğlu, U., Mofjeld, H., Synolakis, C. E., ... and Horning, T.: Probabilistic tsunami hazard assessment at seaside, Oregon, for near-and far-field seismic sources, *Journal of Geophysical Research: Oceans* 114(C11), <https://doi.org/10.1029/2008JC005132>, 2009.



- Gonzalez, F. I., LeVeque, R. J., and Adams, L. M.: Probabilistic Tsunami Hazard Assessment (PTHA) for Crescent City, CA. Final Report for Phase I. University of Washington Department of Applied Mathematics, 565 <http://hdl.handle.net/1773/25916>, 2013.
- Hancilar, U.: Identification of elements at risk for a credible tsunami event for Istanbul, Nat. Hazards Earth Syst. Sci., 12, 107-119, <https://doi.org/10.5194/nhess-12-107-2012>, 2012.
- Hergert, T., and Heidbach, O.: Slip-rate variability and distributed deformation in the Marmara Sea fault system, Nature Geoscience, 3(2) 132, <https://doi.org/10.1038/ngeo739>, 2010.
- 570 Imamura, F.: Tsunami Numerical Simulation with the Staggered Leap-frog Scheme (Numerical code of TUNAMI-N1), School of Civil Engineering, Asian Institute Technical and Disaster Control Research Center, Tohoku University, Tohoku, 1989.
- Imamura, F., A.C. Yalçiner, A. C. and G. Özyurt, TUNAMI-N2: Tsunami Modelling Manual, 2001.
- Imren, C., Le Pichon, X., Rangin, C., Demirbağ, E., Ecevitoglu, B., and Görür, N.: The North Anatolian Fault within the Sea of Marmara: a new interpretation based on multi-channel seismic and multi-beam bathymetry data, Earth and Planetary Science Letters 186(2) 143-158, [https://doi.org/10.1016/S0012-821X\(01\)00241-2](https://doi.org/10.1016/S0012-821X(01)00241-2), 2001.
- Insel, I., The Effects of the Material Density and Dimensions of the Landslide on the Generated Tsunamis, Mcs.Thesis, Middle East Technical University, Ankara, Turkey, 2009.
- Jonkman, S. N., and Penning-Rowsell, E.: Human instability in Flood Flows, JAWRA Journal of the American Water Resources Association, 44.5, 1208-1218, <https://doi.org/10.1111/j.1752-1688.2008.00217.x>, 2008.
- 580 Karabulut, H., Bouin, M. P., Bouchon, M., Dietrich, M., Cornou, C., and Aktar, M.: The seismicity in the eastern Marmara Sea after the 17 August 1999 Izmit earthquake, Bulletin of the Seismological Society of America, 92(1), 387-393, <http://dx.doi.org/10.1785/0120000820>, 2002.
- Karabulut, H., Özalaybey, S., Taymaz, T., Aktar, M., Selvi, O., and Kocaoğlu, A.: A tomographic image of the shallow crustal structure in the Eastern Marmara, Geophysical research letters, 30(24), <https://doi.org/10.1029/2003GL018074>, 2003.
- 585 Kanamori, H.: The diversity of the physics of earthquakes, Proceedings of the Japan Academy, Series B, 80(7) 297-316, <https://doi.org/10.2183/pjab.80.297>, 2004.
- Le Pichon, X., Şengör, A. M. C., Demirbağ, E., Rangin, C., Imren, C., Armijo, R., ..and Saatçılar, R.: The active main Marmara fault, Earth and Planetary Science Letters 192(4), 595-616, [https://doi.org/10.1016/S0012-821X\(01\)00449-6](https://doi.org/10.1016/S0012-821X(01)00449-6), 2001.
- 590 Le Pichon, X., Chamot-Rooke, N., Rangin, C., and Şengör, A. M. C.: The North Anatolian fault in the sea of Marmara, Journal of Geophysical Research Solid Earth 108(B4), <https://doi.org/10.1029/2002JB001862>, 2003.
- Le Pichon, X., Şengör, A. C., Kende, J., İmren, C., Henry, P., Grall, C., and Karabulut, H.: Propagation of a strike-slip plate boundary within an extensional environment: the westward propagation of the North Anatolian Fault, Canadian Journal of Earth Sciences, 53(11) 1416-1439, <https://doi.org/10.1139/cjes-2015-0129>, 2015.
- 595 Lynett, P. J., Gately, K., Wilson, R., Montoya, L., Arcas, D., Aytore, B., and David, C. G.: Inter-model analysis of tsunami-induced coastal currents, Ocean Modelling 114 14-32, <https://doi.org/10.1016/j.ocemod.2017.04.003>, 2017.
- Meade, B. J., Hager, B. H., McClusky, S. C., Reilinger, R. E., Ergintav, S., Lenk, O., ... and Ozener, H.: Estimates of seismic potential in the Marmara Sea region from block models of secular deformation constrained by Global Positioning System measurements, Bulletin of the Seismological Society of America, 92(1) 208-215, 600 <https://doi.org/10.1785/0120000837>, 2002.
- McNeill, L. C., Mille, A., Minshull, T. A., Bull, J. M., Kenyon, N. H., and Ivanov, M.: Extension of the North Anatolian Fault into the North Aegean Trough: Evidence for transtension, strain partitioning, and analogues for Sea of Marmara basin models, Tectonics 23(2), <https://doi.org/10.1029/2002TC001490>, 2004.
- Murru, M., Akinci, A., Falcone, G., Pucci, S., Console, R., and Parsons, T.: $M \geq 7$ earthquake rupture forecast and time-dependent probability for the Sea of Marmara region Turkey, Journal of Geophysical Research: Solid Earth 121(4) 2679-2707, <https://doi.org/10.1002/2015JB012595>, 2016.
- 605 NAMI DANCE: Manual of Numerical Code NAMI DANCE, published in <http://namidance.ce.metu.edu.tr>, 2011.
- NTHMP, Proceedings and Results of the National Tsunami Hazard Mitigation Program 2015 Tsunami Current Modeling Workshop, Portland, Oregon, 2015.
- 610 Okada, Y.: Surface deformation due to shear and tensile faults in a half-space, Bulletin of the seismological society of America, 75(4) 1135-1154, 1985.



- Okay, A. I., Demirbağ, E., Kurt, H., Okay, N., and Kuşçu, İ.: An active, deep marine strike-slip basin along the North Anatolian fault in Turkey, *Tectonics* 18(1) 129-147, <https://doi.org/10.1029/1998TC900017>, 1999.
- 615 Ozer Sozdinler, C., O. Necmioglu, Bayraktar H. B. and Ozel N.M.: Tectonic Origin Tsunami Scenario Database for the Marmara Region, *Nat. Hazards Earth Syst. Sci.*, Manuscript submitted for publication, 2019.
- Parsons, T.: Recalculated probability of $M \geq 7$ earthquakes beneath the Sea of Marmara, Turkey, *Journal of Geophysical Research: Solid Earth* 109(B5), <https://doi.org/10.1029/2003JB002667>, 2004.
- Pondard, N., Armijo, R., King, G. C., Meyer, B., and Flerit, F.: Fault interactions in the Sea of Marmara pull-apart (North Anatolian Fault): earthquake clustering and propagating earthquake sequences, *Geophysical Journal International* 171(3) 1185-1197, <https://doi.org/10.1111/j.1365-246X.2007.03580.x>, 2007.
- 620 Reilinger, R., McClusky, S., Vernant, P., Lawrence, S., Ergintav, S., Cakmak, R., ... and Nadariya, M.: GPS constraints on continental deformation in the Africa-Arabia-Eurasia continental collision zone and implications for the dynamics of plate interactions, *Journal of Geophysical Research: Solid Earth* 111(B5), <https://doi.org/10.1029/2005JB004051>, 2006.
- Shuto, N., Goto, C., and Imamura, F.: Numerical simulation as a means of warning for near-field tsunamis, *Coastal Engineering in Japan*, 33(2) 173-193, <https://doi.org/10.1080/05785634.1990.11924532>, 1990.
- 625 Sørensen, M. B., Spada, M., Babeyko, A., Wiemer, S., and Grünthal, G.: Probabilistic tsunami hazard in the Mediterranean Sea, *Journal of Geophysical Research: Solid Earth* 117(B1), <https://doi.org/10.1029/2010JB008169>, 2012.
- Stein, R. S., Barka, A. A., and Dieterich, J. H.: Progressive failure on the North Anatolian fault since 1939 by earthquake stress triggering, *Geophysical Journal International* 128(3), 594-604, <https://doi.org/10.1111/j.1365-246X.1997.tb05321.x>, 1997.
- 630 Synolakis, C. E., Bernard, E. N., Titov, V. V., Kânoğlu, U., and González, F. I.: Standards, Criteria, and Procedures for NOAA Evaluation of Tsunami Numerical Models, 2007.
- Synolakis, C. E., Bernard, E. N., Titov, V. V., Kânoğlu, U., and Gonzalez, F. I.: Validation and verification of tsunami numerical models. In *Tsunami Science Four Years after the 2004 Indian Ocean Tsunami*, pp. 2197-2228, Birkhäuser, Basel, 2008.
- 635 Takagi, H., Mikami, T., Fujii, D., Esteban, M., and Kurobe, S.: Mangrove forest against dyke-break-induced tsunami on rapidly subsiding coasts, *Nat. Hazards Earth Syst. Sci.*, 16, 1629-1638, <https://doi.org/10.5194/nhess-16-1629-2016>, 2016.
- Velioglu, D., *Advanced Two and Three Dimensional Tsunami Models: Benchmarking and Validation*, Msc. Thesis, Middle East Technical University, Ankara, Tukey, 2009.
- 640 Wells, D. L., and Coppersmith, K. J.: New empirical relationships among magnitude, rupture length, rupture width, rupture area, and surface displacement., *Bulletin of the seismological Society of America*, 84(4), 974-1002, 1994.
- Wessel, P., and Smith, W. H.: New, improved version of Generic Mapping Tools released, *Eos, Transactions American Geophysical Union*, 79(47), 579-579, <https://doi.org/10.1029/98EO00426>, 1998.
- WGCEP (Working Group on California Earthquake Probabilities): Earthquake probabilities in the San Francisco Bay region: 2002–2031, US Geological Survey Open-File Report 03-214, 2003.
- 645 Wong, H. K., Lüdmann, T., Ulug, A., and Görür, N.: The Sea of Marmara: a plate boundary sea in an escape tectonic regime, *Tectonophysics* 244(4) 231-250, [https://doi.org/10.1016/0040-1951\(94\)00245-5](https://doi.org/10.1016/0040-1951(94)00245-5), 1995.
- Yalciner, A. C., Synolakis, C., Borrero, J., Altinok, Y., Watts, P., Imamura, F., ... and Tinti, S.: Tsunami generation in Izmit Bay by the 1999 Izmit earthquake, *Conference on the 1999 Kocaeli Earthquake*, pp. 217-221, Istanbul Technical University, Istanbul, Turkey, 1999.
- 650 Yalciner, A. C., Altinok, Y., Synolakis, C. E., Borrero, J., Imamura, F., Ersoy, S., ... and Yuksel, Y.: Tsunami waves in İzmit Bay, *Earthquake Spectra* 16(S1), 55-62, 2000.
- Yalçiner, A. C., Alpar, B., Altinok, Y., Özbay, İ., and Imamura, F.: Tsunamis in the Sea of Marmara: Historical documents for the past, models for the future, *Marine Geology* 190(1-2), 445-463, [https://doi.org/10.1016/S0025-3227\(02\)00358-4](https://doi.org/10.1016/S0025-3227(02)00358-4), 2002.
- 655 Yaltrak, C.: Tectonic evolution of the Marmara Sea and its surroundings, *Marine Geology* 190(1-2), 493-529, [https://doi.org/10.1016/S0025-3227\(02\)00360-2](https://doi.org/10.1016/S0025-3227(02)00360-2), 2002.
- Zolfaghari, M. R.: Development of a synthetically generated earthquake catalogue towards assessment of probabilistic seismic hazard for Tehran, *Natural Hazards*, 76(1), 497-514, <https://doi.org/10.1007/s11069-014-1500-1>, 2015.